Molar Mass Distribution and Solubility Modeling of Asphaltenes

Harvey W. Yarranton and Jacob H. Masliyah
Dept. of Chemical Engineering, University of Alberta, Edmonton, Alberta, Canada, T6G 2G6

Attempts to model asphaltene solubility with Scatchard-Hildebrand theory were hampered by uncertainty in molar volume and solubility parameter distribution within the asphaltenes. By considering asphaltenes as a series of polyaromatic hydrocarbons with randomly distributed associated functional groups, molar volume and solubility parameter distributions are calculated from experimental measurements of molar mass and density. The molar mass distribution of Athabasca asphaltenes is determined from interfacial tension and vapor pressure osmometry measurements together with plasma desorption mass spectrometry determinations from the literature. Asphaltene densities are calculated indirectly from mixtures of known concentration of asphaltene in toluene. Asphaltene density, molar volume, and solubility parameter are correlated with molar mass. Solid-liquid equilibrium calculations based on solubility theory and the asphaltene property correlations successfully predict experimental data for both the precipitation point and the amount of precipitated asphaltenes in toluene-hexane solvent mixtures.

Introduction

Crude oils are a complex mixture of hydrocarbons which, for convenience, are divided into several classes of material. In order of increasing polarity, the classes are: saturates, aromatics, resins, and asphaltenes. Asphaltenes are the fraction of an oil that is soluble in toluene and insoluble in an alkane, typically pentane or heptane. Asphaltenes are of interest in many aspects of oil production, because they tend to precipitate under producing conditions and can stabilize water-in-oil emulsions. However, since they are defined as a solubility class which consists of a large variety of molecules, they are difficult to characterize.

Asphaltenes are generally considered to be polyaromatic hydrocarbons, consisting primarily of aromatic and aliphatic groups (approximately 89% by mass) along with a variety of associated functional groups, including acids, thiophenes, pyridines, and porphyrins (Strausz et al., 1992; Speight and Moschopedis, 1979). Recent work has demonstrated that, while there is a broad range of molar masses in the asphaltene fraction, roughly from 1,000 to 10,000+g/mol, the functionality of the molecules does not vary significantly (Cyr et al., 1987; Anderson, 1994), although there is some evidence that the functional groups tend to concentrate slightly at the upper end of the molar mass distribution (Brons, 1995). In most cases, the aromaticity of the asphaltenes was found to increase with increasing molar mass. To summarize, asphaltenes can be approximated as a series of polyaromatic hydrocarbons of increasing molar mass and aromaticity with a variety of associated functional groups randomly distributed on a mass basis.

In attempting to describe the solubility of asphaltenes, most approaches have adopted some form of Scatchard-Hildebrand solubility theory (Cimino et al., 1995), although in many cases the asphaltenes have been treated as a uniform material (Hirschberg et al., 1984). While these models have successfully predicted the precipitation point, they have been less successful in predicting the amount of precipitated material. It has been recently shown that more accurate results can be obtained when the ranges of molar volume and solubility parameter are accounted for with a solid-liquid equilibrium method (Kawanaka et al., 1991; Ferworn and Svercek, 1994). The last approach has been particularly successful with wax precipitation where the physical properties of the wax are reasonably well-known (Lira-Galeana et al., 1996). However, because the physical properties of the asphaltenes are difficult to measure they are generally approximated using equations of state (Thomas et al., 1992; Rassamdana et al., 1996).

Hence, the usefulness of solubility theory is limited by the accuracy of the molar volume and solubility parameter estimates.

The necessary experimental data to determine molar volume of the asphaltenes are the molar mass and density distributions. Historically, measuring the molar mass distribution has been problematic because asphaltenes self-associate to different degrees in different solvents. Hence, many methods have measured molar masses of asphaltene "micelles" rather than asphaltene molecules. Reasonably good results have been obtained with vapor pressure osmometry (VPO) (Moschopedis et al., 1976) and, recently, plasma desorption mass spectrometry (PDMS) (Larsen and Li, 1995). However, in the former case, the error is sufficiently high that it is difficult to obtain an accurate distribution from a set of asphaltene subfractions. In the latter case, specialized equipment is required and, while the relative distribution seems reasonable, there remains some question as to the absolute value of the molar mass.

In the following study, a series of mass subfractions of Athabasca asphaltene is obtained by solvent extraction. The molar masses of the subfractions are determined from interfacial tension data and compared with VPO values. The resulting distribution is compared with PDMS measurements from the literature and used as the basis for a solid-liquid equilibrium model for the asphaltenes. Asphaltene densities are determined indirectly from measurements of asphaltene-toluene solution densities. Correlations based on molar mass are developed from the experimental molar mass and density data for the two key model parameters, molar volume and solubility parameter. The model is tested on solubility measurements in toluene-hexane mixtures.

Experimental Method

Terminology

Asphaltenes are defined as the crude oil constituents that are insoluble in an alkane but soluble in toluene. When asphaltenes are precipitated from a crude oil, some other material also precipitates. This other material, the "solids," includes ash, fine clays, and some adsorbed hydrocarbons and is insoluble in toluene. The mixture of asphaltenes and solids that first precipitates shall be referred to as "asphaltene-solids." (A superscript * will be added to symbols that apply to asphaltene-solids to distinguish them from symbols applying to solids-free asphaltenes. The asphaltene-solids precipitated directly from the bitumen will be referred to as the asphaltene-solids fraction. Any material separated from the asphaltene-solids fraction will be designated an asphaltene-solids subfraction. Hence, during a precipitation, the asphaltene-solids fraction is separated into a soluble subfraction and an insoluble subfraction. Whenever asphaltenes are referred to without the "-solids" modifier, it means that the asphaltenes are free of solids.)

Materials

Asphaltene-solids were extracted from Syncrude coker feed Athabasca bitumen (bitumen that has been treated to remove sand and water and is ready for upgrading) with a 40:1 vol. ratio of heptane:bitumen. The mixture was stirred for 4 h and left to settle overnight. Then, the supernatant liquid was removed and the remaining precipitate further diluted with heptane at a 4:1 vol. ratio heptane:bitumen. After 4 h, the final mixture was filtered and the remaining asphaltene-solids precipitate dried at ambient conditions until there was no further change in mass. The drying usually required one week. The asphaltene-solids recovered with this method made up 14.5 wt. % of the original bitumen. Reagent grade toluene, hexane, and heptane were purchased from Fischer Scientific. Demineralized water produced by reverse osmosis was used for all interfacial tension measurements.

Asphaltene-solids subfractions were obtained with solvent extraction in two ways: by solubility and by precipitation. For the solubility method, asphaltene-solids were added to a premixed known ratio of hexane and toluene. The solution was stirred in a sonic mixer for 10 min (20 min at high asphaltene concentrations), left for 24 h and then centrifuged at 3,400 rpm for 5 min. The supernatant liquid was poured off and the undissolved asphaltene-solids subfraction dried until there was no further change in mass. For the precipitation method, the procedure was identical except that the asphaltene-solids were dissolved in toluene before the hexane was added. In the first case, the undissolved portion of the asphaltene-solids was recovered and in the second case, the precipitated portion.

In order to measure true asphaltene properties, the solids must be removed. When required, the solids were removed with the following procedure. The asphaltene-solids were dissolved in toluene and centrifuged at 3,400 rpm for 5 min. The supernatant liquid was recovered and evaporated until only dry asphaltene remained. In the case of asphaltene subfractions, the supernatant liquid was used in the precipitation solvent extraction method described above.

Density measurements

Densities were measured with an Anton Paar DMA 45 density meter calibrated with demineralized water and toluene. Density measurements with this instrument are generally accurate to ± 0.03 kg/m^3. All measurements were made at 25.7 ± 0.05°C. Asphaltene densities were calculated indirectly from the densities of mixtures of known concentration of asphaltene in toluene.

Interfacial tension measurements

Interfacial tensions of oil over demineralized water were measured with a Fisher deNouy ring tensiometer accurate to ± 0.5 mN/m. For each measurement, the platinum ring was placed in the water, the organic phase was added dropwise to the water surface and the two-phase system left to equilibrate for one hour before the ring was pulled through the interface. Before each measurement, the surface tension of the water was checked and, after each measurement, the ring was cleaned in toluene and any traces of hydrocarbon burned off. All measurements were corrected for the solvent density using the Harkins and Jordan tables (Harkins and Jordan, 1930).

Vapor pressure osmometry

Molar masses were determined with a Westcan Instrument Inc. Model 232A vapor pressure osmometer calibrated with

benzil. Measurements in toluene and 1,2-dichlorobenzene were made at 50 and 120°C, respectively. Asphaltene molar masses in toluene were determined over a range of 1.5 to 4.5 g asphaltene per L solvent. There was no trend of molar mass vs. concentration, so the reported values are an average of two or three measurements. It has been shown previously that asphaltene VPO molar mass is independent of concentration in 1,2-dichlorobenzene at 120°C (Moschopedis et al., 1976). Therefore, in that solvent, only one measurement was taken for each sample.

Theory

Molar mass from interfacial tension measurements

It has already been noted that an estimate of molar mass can be obtained from surface tension data (Taylor, 1992). In a dilute solution, the area that a solute molecule occupies on the interface can be obtained from a plot of surface tension or interfacial tension σ (mN/m) vs. the logarithm of solute concentration C_i (kg/m^3) as follows:

$$\frac{d\sigma}{d\ln C_i} = -RT\Gamma_i = -\frac{RT}{A_i} \tag{1}$$

where R is the gas constant (J/mol·K), T is temperature (K), Γ is molar surface coverage (mmol/m^2), and A_i is molar surface area of the solute (m^2/mmol). When the solute concentration is sufficient to saturate the interface, the molar surface area is constant and can be determined from the slope of a plot of interfacial tension vs. the log of the solute concentration. A molecular geometry must be assumed to calculate a molar volume from the molar surface area and then molar mass is found from the density and the molar volume. The molecular geometry is unknown, but can be approximated as spherical or cylindrical. Both geometries give reasonable results but, in this study, the best results were obtained by assuming a cylindrical geometry. Accordingly, molar mass is expressed by

$$M_i = \rho_i t\left\{\frac{-4RT}{\pi(d\sigma/d\ln C_i)}\right\} \tag{2}$$

where M_i and ρ_i are the molar mass (g/mol) and density (kg/m^3) of component i, respectively. Here, it is also assumed that the molar surface area represents the cross-section of the cylindrical molecule.

Accordingly, t is the height of the cylinder, i.e., the thickness of the molecule (nm). The value of t also accounts for any error introduced by the geometry assumptions. Since t is unknown, the interfacial tension method can be used to determine the shape of the asphaltene molar mass distribution but not the absolute value. Hence, the results must be compared with a second method such as VPO to calculate a value for t. Then, a realistic molar mass distribution can be obtained for use in solubility modeling.

Solubility

Recognizing that asphaltenes are a mixture of molecules, the solubility can be determined in a manner analogous to a multicomponent flash calculation. In this case, it is a solid-liquid equilibria and the appropriate equilibrium ratio is given by $K_i = x_i^s/x_i^l$ where x_i^s and x_i^l are the solid-phase and liquid-phase mole fractions of component i, respectively. As discussed elsewhere (Ferworn and Svercek, 1994), the equilibrium ratio at low pressure can be determined by equating the fugacities in each phase and neglecting pressure effects

$$x_i^l\gamma_i^l f_i^{ol} = x_i^s\gamma_i^s f_i^{os} \tag{3}$$

Here γ_i^l and γ_i^s are the activity coefficients of component i in the liquid and solid phase respectively, and f_i^{ol} and f_i^{os} are the standard state fugacities in the liquid phase and the solid phase, respectively. For solid-liquid equilibria, the ratio of the standard state fugacities can be approximated by (Prausnitz et al., 1986)

$$\frac{f_i^{ol}}{f_i^{os}} = \exp\left\{\frac{\Delta H_i^f}{RT}\left(1-\frac{T}{T_i^f}\right)\right\} \tag{4}$$

where ΔH_i^f is the enthalpy of fusion (J/mol) and T_i^f is the melting point temperature of component i. For low asphaltene concentrations, the activity coefficients can be estimated using Scatchard-Hildebrand solubility theory. With large molecules like asphaltenes, it is necessary to use the Flory-Huggins term for the entropy of mixing molecules with largely different sizes. The resulting expression is given here for the liquid-phase activity coefficient

$$\gamma_i^l = \exp\left\{1-\frac{v_i^l}{v_m}+\ln\left(\frac{v_i^l}{v_m}\right)+\frac{v_i^l}{RT}(\delta_m-\delta_i^l)^2\right\} \tag{5}$$

where v_i^l and v_m are the liquid phase molar volumes (m^3/mol) of component i and the solvent respectively, and δ_i^l and δ_m are the solubility parameters (MPa$^{1/2}$) for the same respective constituents. The solubility parameter is defined as follows

$$\delta_i^l = \left(\frac{\Delta U^{\text{vap}}}{v_i^l}\right)^{1/2} \tag{6}$$

where ΔU^{vap} is the internal energy (J/mol) of vaporization. Note that for asphaltenes, the activity coefficients in the solid phase are near unity especially for the fractions nearest the point of incipient precipitation. Therefore, assuming a value of unity for the solid-phase activity coefficients does not introduce significant error. When Eqs. 4 and 5 are substituted into Eq. 3, the resulting expression for the K-value of component i becomes

$$K_i = \exp\left\{\frac{\Delta H_i^f}{RT}\left(1-\frac{T}{T_i^f}\right)+1-\frac{v_i^l}{v_m}+\ln\left(\frac{v_i^l}{v_m}\right)+\frac{v_i^l}{RT}(\delta_m-\delta_i^l)^2\right\} \tag{7}$$

The properties of most solvents are already known. In order to apply the equilibrium model, it remains to determine the molar volume and solubility parameters of the asphaltenes and to consider the enthalpy of fusion term.

Results and Discussion

It is important to recognize that the asphaltenes precipitated from bitumen contain some other insoluble material (the "solids") and that this material can affect measurements of asphaltene properties. The amount of solids in the asphaltene-solids subfractions is shown in Figure 1. The solids make up 6.3% of the asphaltene-solids fraction or 0.9% of the coker feed bitumen. The same total amount of solids precipitates with each asphaltene-solids subfraction and, therefore, the relative fraction of solids increases as the size of the subfraction decreases. Consequently, the solids can introduce significant error in measurements of the properties of the smallest subfractions.

Solubility data

The solubility of the asphaltene-solids was measured in hexane-toluene solutions of 20, 25, 33, 40 and 50 vol. % toluene. Both the solubility and the precipitation methods give similar results except at low asphaltene concentrations, as shown in Figure 2. At low concentrations, the insoluble subfraction from the precipitation method is smaller probably because flocculation is limited under these conditions. Note, that when used for asphaltene property correlations, the mass fractions in Figure 2 must be adjusted to remove the solids contribution. ϕ_T in Figure 2 is the volume fraction of toluene.

Figure 2 also illustrates that the fraction of asphaltene-solids that precipitates at a given volume fraction of toluene is virtually independent of asphaltene concentration from

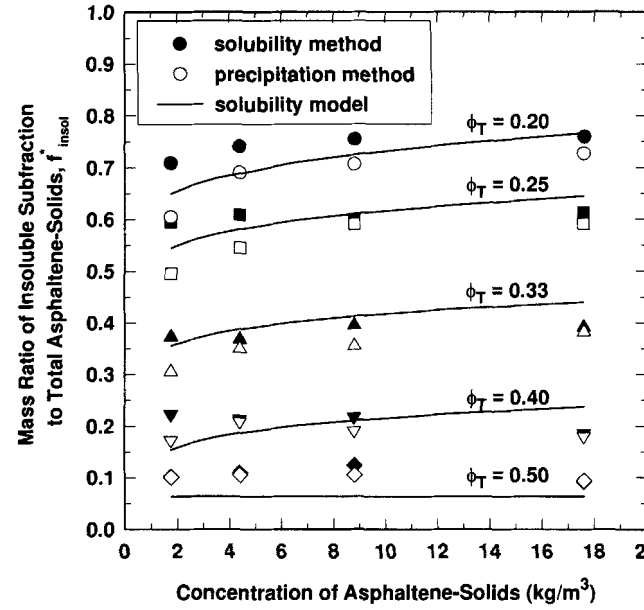

Figure 2. Effect of asphaltene concentration on solubility of asphaltene-solids in solutions of toluene and hexane.

concentrations of 1.76 to 17.6 kg/m^3. It is interesting to compare Figure 2 with the solubility curve of a pure component given in Figure 3. The solute concentration in Figure 3 is normalized to the precipitation point concentration. Figure 3 shows that at normalized concentrations greater than 10, the insoluble mass fraction is greater than 0.85. Returning to Figure 2, the precipitation point concentration is unknown but, since precipitation occurred at all concentrations, it must be less than the lowest experimental asphaltene concentration,

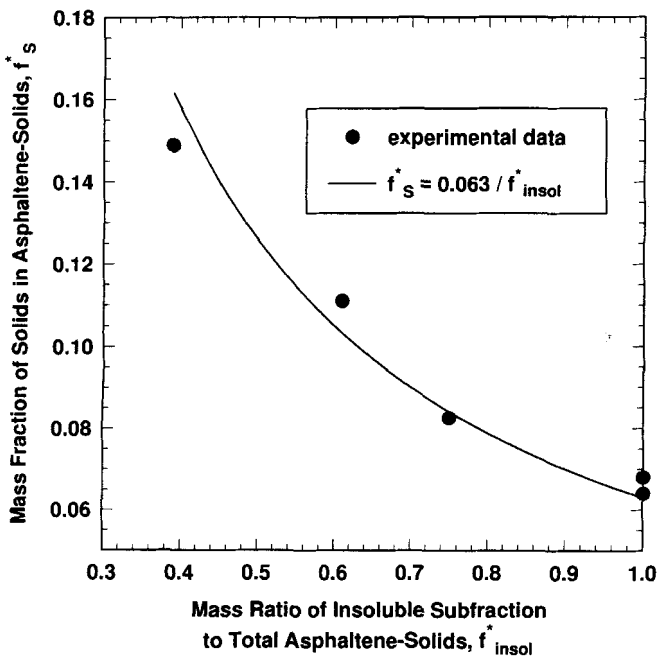

Figure 1. Mass fraction of solids in asphaltene-solids subfractions.

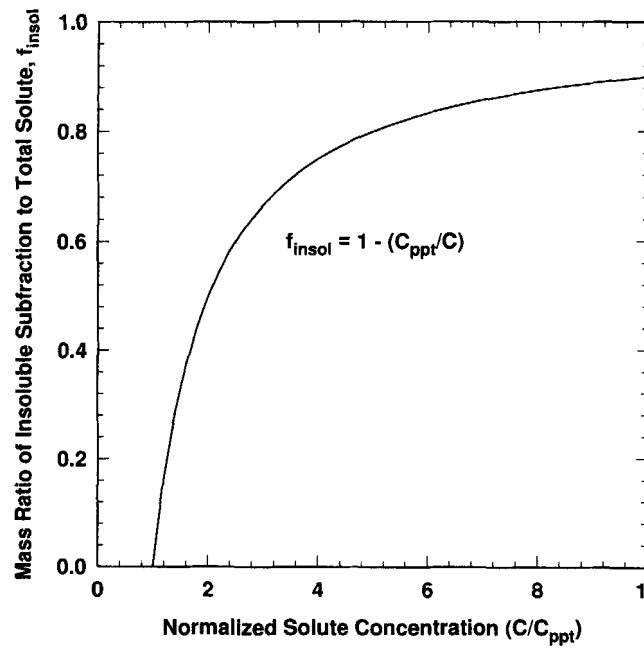

Figure 3. Theoretical solubility of pure solute as function of solute concentration.

1.76 kg/m^3. Hence, the highest experimental asphaltene concentration of 17.6 kg/m^3 corresponds to a normalized concentration of at least 10. If the asphaltenes acted as a pure component, the insoluble mass fraction at 17.6 kg/m^3 of asphaltene should be greater than 0.85. This is not the case and therefore asphaltenes cannot be considered as a uniform solubility class, but must rather be treated as a range of molecular species.

Now, as will be shown, the higher the asphaltene molar mass, the less soluble it is. Also, by definition, all the asphaltenes are soluble in toluene but insoluble in hexane. Therefore, the higher the toluene/hexane ratio, the less asphaltene precipitates and the higher the molar mass and density of the precipitated subfraction. Consequently, the series of increasing toluene/hexane ratios yield a series of asphaltene subfractions with increasing molar mass and density from which the desired molar mass and density distributions can be calculated.

Density

Densities were measured for solutions of asphaltene in toluene at asphaltene concentrations of 0 to 1.14 wt. %. Experiments were carried out on the entire asphaltene fraction and on the insoluble subfractions precipitated from hexane-toluene solutions of 20, 25, and 33 vol. % toluene. Fractions with and without the solids were examined.

At low concentration, regular solution behavior can be assumed. Consequently, the asphaltene density can be determined indirectly from a plot of the inverse mixture density vs. asphaltene mass fraction, as follows

$$\frac{1}{\rho_M} = \frac{1}{\rho_T} + \left(\frac{1}{\rho_A} - \frac{1}{\rho_T}\right) x_A \tag{8}$$

hence

$$\rho_A = \frac{1}{S + I} \tag{9}$$

where ρ_M, ρ_T and ρ_A are the mixture, toluene and average asphaltene densities (kg/m^3), respectively, and x_A is the asphaltene mass fraction. S and I are the slope and intercept of the inverse mixture density plot, respectively. Similarly, if the density of the solids is known, the average density of the asphaltenes can be estimated from a plot of inverse mixture density vs. mass fraction of the asphaltene-solids

$$\rho_A = \frac{1}{\dfrac{S^*}{1 - f_S^*} + (1 + f_S^*) I^* - \dfrac{f_S^*}{\rho_S}} \tag{10}$$

where ρ_S is the density of the solids, f_S^* is the mass fraction of solids in the asphaltene-solids mixture. S^* and I^* are the slope and intercept of the inverse mixture density vs. mass fraction asphaltenes-solid plot.

A typical mixture density plot is given in Figure 4. The calculated average asphaltene densities are shown in Figure 5. Corrected values from the asphaltene-solids data were obtained using Eq. 10 and a solids density of 1,550 kg/m^3. This

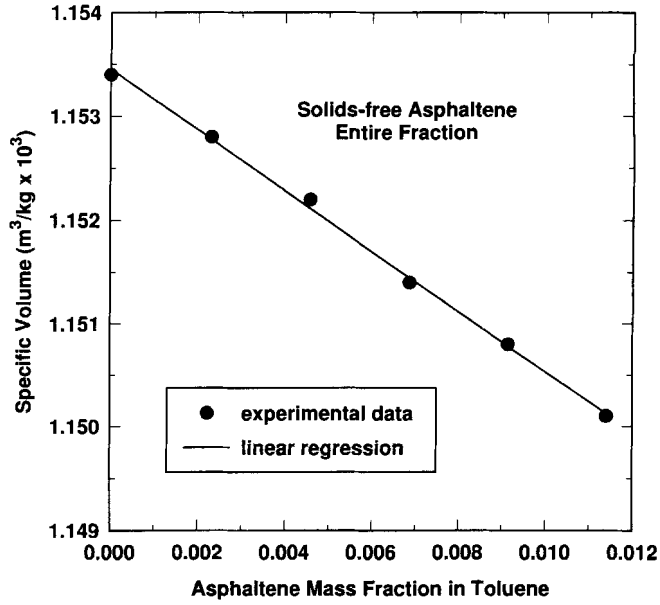

Figure 4. Dependence of asphaltene-toluene mixture density on asphaltene concentration.

value is consistent with the expectation that the solids are comprised of ash, clay fines, and adsorbed hydrocarbons. The average density varies only 5% for $0.35 < f_{insol} \leq 1.0$. Such a narrow change in density contributes to the apparent scatter in Figure 5 even though the deviation is within 1%. Although the density data are scattered, a downward trend is evident. Therefore, a constant density or zero-order density model is inappropriate. However, the density determinations are not accurate enough to justify fitting the data with more than a first-order model. Consequently, we assume that asphaltene density increases linearly with molar mass. As will be dis-

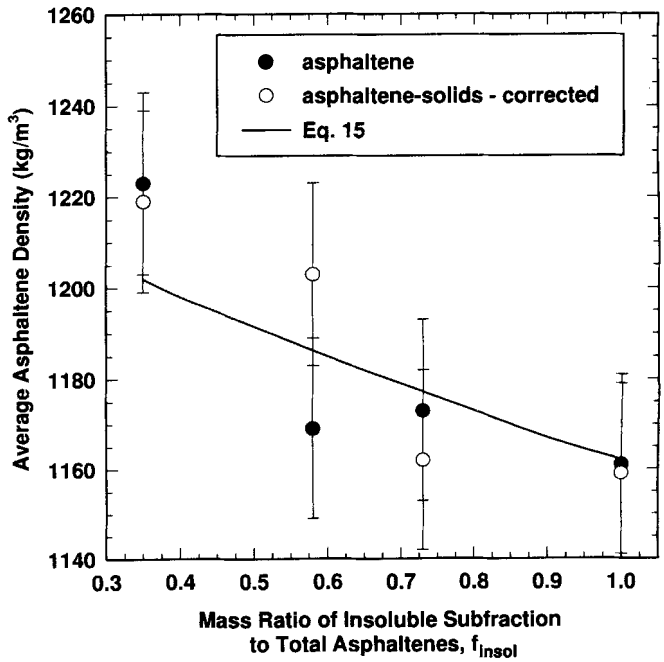

Figure 5. Average density of asphaltene subfractions.

cussed later, molar mass is related to the mass frequency distribution as follows

$$F_i = \frac{df_i}{dM_i} = \text{constant}\,(1 + \alpha \exp\{-\beta M_i\}) \tag{11}$$

where α and β have values of 50.63 and 0.00165 mol/g, respectively, and are used to fit the molar mass distribution. F_i and M_i are the mass frequency and molar mass, respectively, of the ith asphaltene component. f_i is the cumulative mass frequency up to the ith asphaltene component. Equation 11 can be integrated to find the cumulative mass frequency, given in Eq. 12

$$\int_{M_L}^{M_i}\left(\frac{df_i}{dM_i}\right)dM_i = f_i = f_{\text{sol}} = \frac{M_i - M_L - \alpha(\exp\{-\beta M_i\} - \exp\{-\beta M_L\})}{M_H - M_L - \alpha(\exp\{-\beta M_H\} - \exp\{-\beta M_L\})} \tag{12}$$

Here f_{sol} is the mass ratio of the lightest asphaltene subfraction to the total asphaltene fraction. f_{sol} is expected to be equivalent to f_i. M_L and M_H are the molar masses of the smallest and largest asphaltene components, respectively. Now, the average density of the insoluble asphaltene subfraction in terms of f_i is given by

$$\bar{\rho}_{\text{insol}} = \frac{\int_{f_{\text{sol}}}^{1} df_i}{\int_{f_{\text{sol}}}^{1} \frac{df_i}{\rho_i}} \tag{13}$$

However, Eq. 13 is more easily solved in terms of molar mass. Given that

$$\rho_i = aM_i + b \tag{14}$$

the average density of the insoluble subfraction may be expressed as follows

$$\bar{\rho}_{\text{insol}} = \frac{M_H - M_i - \frac{\alpha}{\beta}(\exp\{-\beta M_H\} - \exp\{-\beta M_i\})}{\int_{M_i}^{M_H}\left(\frac{1 + \alpha\exp\{-\beta M_i\}}{\alpha M_i + b}\right)dM_i} \tag{15}$$

Similarly, the average density of the soluble subfraction is given by

$$\bar{\rho}_{sol} = \frac{M_i - M_L - \frac{\alpha}{\beta}(\exp\{-\beta M_i\} - \exp\{-\beta M_L\})}{\int_{M_L}^{M_i}\left(\frac{1 + \alpha\exp\{-\beta M_i\}}{\alpha M_i + b}\right)dM_i} \tag{16}$$

Here, ρ_i is the density of the ith asphaltene component and $\bar{\rho}_{\text{insol}}$ and $\bar{\rho}_{\text{sol}}$ are the average densities of the insoluble (high molar mass) and soluble (low molar mass) asphaltene subfractions, respectively. a and b are the linear fit coefficients of the asphaltene density to molar mass. Values of 0.017 and 1,080 for a and b respectively were estimated to provide the best fit of the solubility data later on. As will be discussed later, values of 2,000 and 8,500 g/mol were determined for M_L and M_H, respectively. To compare calculated average densities with experimental data, Eq. 12 was used to determine the M_i that corresponds to a given f_{sol}. Then Eq. 15 was solved numerically with M_i serving as the lower integration limit. Average densities predicted from Eq. 15 are compared with the experimental data in Figure 5.

The scatter in the density determinations illustrates the difficulty in obtaining asphaltene density distributions and may explain why there is little data on asphaltene densities in the literature. However, a value of 1,158 kg/m^3 was predicted by Mehrotra et al. (1995) for a fraction of Athabasca bitumen making up 20 wt. % of the bitumen and containing the densest constituents. Their value of 1,158 kg/m^3 compares well with our experimental average density of 1,162 kg/m^3 for the entire asphaltene fraction, which comprises 14.5 wt. % of the bitumen.

Interfacial tension and molar mass

The near independence of solubility on asphaltene concentration, demonstrated in Figure 2, proved useful for the interpretation of the interfacial tension data. For a solution where only part of the asphaltenes is soluble, the slope in Eq. 1 can be expressed as

$$\frac{d\sigma}{d\ln C_i^{sol}} = \frac{d\sigma}{d\ln(f_{\text{sol}}^{*} C_i)} \tag{17}$$

where C_i^{sol} is the concentration of the soluble fraction of the asphaltene. As long as f_{sol}^{*} is constant, Eq. 17 is equivalent to the slope used in Eq. 1. Therefore, a plot of interfacial tension vs. the concentration of asphaltene-solids mixture gives the correct slope for use in Eq. 2.

It is also necessary to determine if the precipitated asphaltenes affect the interfacial tension measurements. Measurements with and without the precipitated material are compared in Figure 6. The presence of precipitated asphaltenes has no effect on the results at concentrations below 2 kg/m^3. Above 2 kg/m^3, the precipitate leads to higher interfacial tension values. At high concentrations, the precipitate may change the local density and lead to errors in the deNouy ring density correction or perhaps mechanically strengthen the interface. Note in Figure 6 that, for the purpose of comparison, the concentration of asphaltene prior to the removal of precipitate was used.

Interfacial tensions were measured for asphaltenes in toluene-hexane solutions of 20, 25, 33, 40, 50 and 100 vol. % toluene. The following properties were calculated from the interfacial tension data and are listed in Table 1: the slope for Eq. 1, molecular cross section, molar mass. The mass ratio of the soluble subfractions to the entire asphaltene fraction given in Table 1 were corrected to account for the contribution of the solids. The asphaltene densities given in Table 1 apply to the soluble portion of the asphaltenes and were calculated numerically from Eq. 16. Molecular cross sections are the ratio of molar surface area to Avogadro's number. A

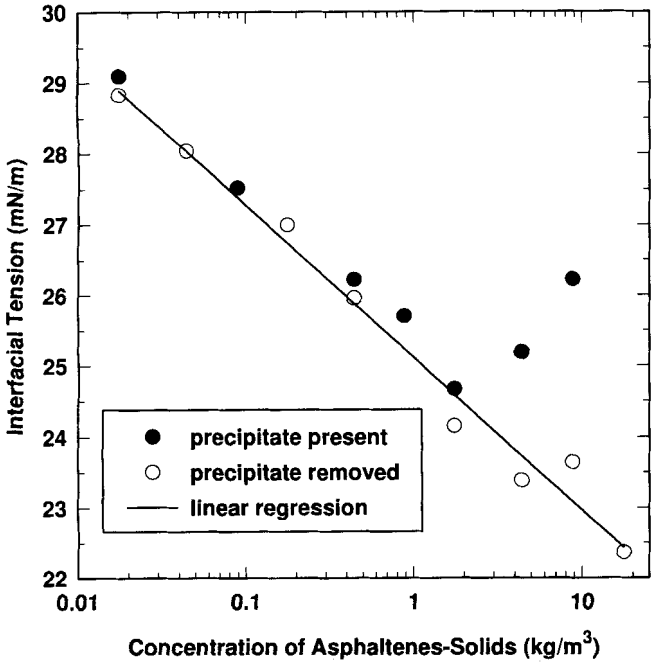

Figure 6. Interfacial tension of asphaltene-solids in toluene-hexane solution of 25 vol. % toluene over water.

value of 1.18 nm was estimated for t and it will be discussed later. The molecular cross sections are in good agreement with those calculated from surface tension data (Taylor, 1992; Sheu et al., 1992). The calculated molar mass decreases from 3,900 g/mol for the entire asphaltene fraction to 2,600 g/mol for the smallest soluble subfraction. A question arises: do the molar mass values represent the average of the molecules in solution or only of the highest molar mass, possibly the most surface active, when the fraction is still soluble?

To answer the question, the interfacial area of a high molar mass subfraction must be compared with that of the entire asphaltene fraction, each in a solvent where both are fully soluble. If the interface is dominated by the highest molar mass molecules still in solution, the measured molar surface area should be the same in both cases. If the interface is covered by a representative mixture of molecules, the molar surface areas should reflect the average molar mass of the subfractions. A high molar mass asphaltene fraction was precipitated from bitumen with the procedure described in the materials section except that a 4:1 volume ratio of heptane to bitumen was used instead of a 40:1 ratio. The resulting fraction made up 10.0% of the bitumen by mass and 69% of the fraction precipitated at the 40:1 ratio. Accounting for the solids, the 4:1 fraction contains 65% of the asphaltene in the 40:1 fraction. Interfacial tensions were measured for the 4:1 fraction in toluene and compared with the results for the 40:1 fraction, as shown in Figure 7 and Table 1. The calculated molar mass of the 4:1 fraction is 70% greater than that of the 40:1 sample. Hence, the measured molar surface area and the corresponding molar mass more closely reflect the average properties of the molecules in solution rather than the properties of a particular subfraction.

Table 1. Molar Masses Calculated from Interfacial Tension Data

Vol. % Toluene in Solvent	f_{sol} (Mass %)	$\frac{d\sigma}{d \ln C_A}$ (mN/m)	Molecular Cross-Section $(nm)^2$	Avg. Density (kg/m^3)	Avg. Mol. Mass (g/mol)
20	0.29	−1.2487	3.26	1,123	2,600
25	0.42	−1.1468	3.55	1,129	2,850
33	0.65	−1.0125	4.02	1,141	3,260
40	0.84	−0.9178	4.43	1,152	3,630
50	0.96	−0.9134	4.45	1,159	3,670
100	1.00	−0.8569	4.75	1,162	3,920
100	0.35*	−0.5258	7.75	1,202	6,620

*Asphaltene from the 4:1 precipitation contains 65% of the highest molar mass material from the 40:1 precipitation. Hence, the 4:1 fraction is equivalent to an f_{sol} of 0.35 for the 40:1 sample.

Also of interest here is that in none of the interfacial tension measurements was the asphaltene critical micelle concentration (cmc) reached. Above the cmc, interfacial tension is independent of the surfactant concentration. Thus, the cmc for Athabasca asphaltenes is above 44 kg/m^3 in toluene and 18 kg/m^3 in a toluene-hexane mixture of 25 vol. % toluene. All the measurements reported in this article are taken below the cmc and, therefore, are not influenced by the presence of micelles. In particular, the VPO results in toluene are expected to reflect the molar mass of molecules rather than micelles.

VPO molar masses were obtained for the insoluble asphaltene-solids subfractions precipitated in toluene-hexane solutions of 0, 20, 25, and 33 vol. % toluene. The VPO measurements were made with toluene and 1,2-dichlorobenzene as a solvent, as shown in Figure 8. The values in 1,2-dichlorobenzene are 2.2 times lower than those in toluene. This is somewhat greater than the ratio of 1.6 reported elsewhere (Moschopedis et al., 1976), but ratios as high as 3.6 have been observed with similar solvents (Acevedo et al., 1992). The difference in the apparent asphaltene molar mass in different solvents has been attributed to different degrees of molecular

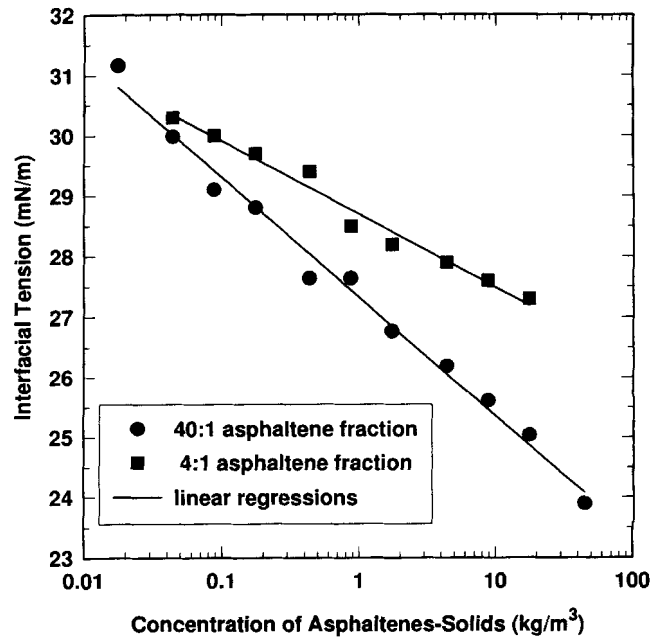

Figure 7. Interfacial tension of solutions of asphaltene-solids in toluene over water.

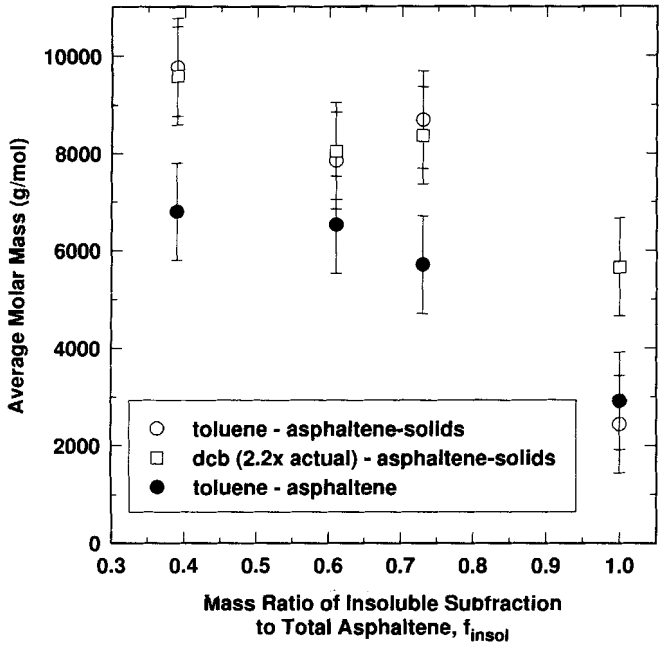

Figure 8. Molar mass of asphaltene subfractions determined by vapor pressure osmometry.

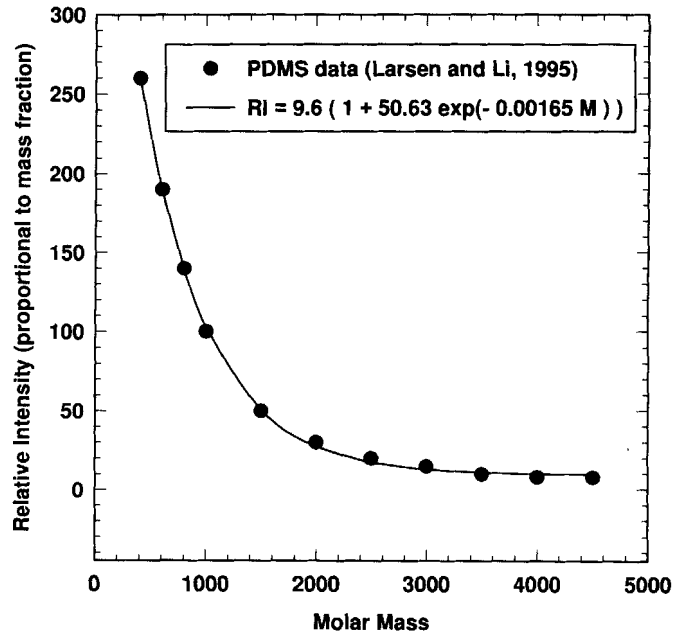

Figure 10. PDMS molar mass frequency distribution of Athabasca bitumen.

stacking (Brandt et al., 1995). Given that the apparent molar mass does not vary with concentration in either case, it may be that the asphaltenes are more fragmented in 1,2-dichlorobenzene solvent than in toluene. For present purposes, the results in toluene will be accepted.

To check on the effect of the solids, VPO measurements using toluene as the solvent were conducted on solids-free samples. As observed in Figure 8, the asphaltene molar masses are roughly 25% lower than the asphaltene-solids samples. Hence, the solids introduce a 25% error. The asphaltene and corrected asphaltene-solids VPO molar masses are compared with the interfacial tension results in Figure 9.

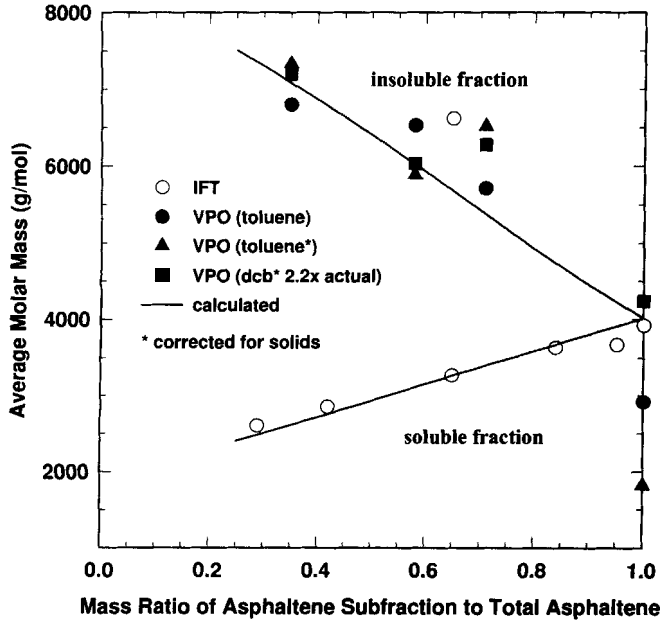

Figure 9. Molar mass of asphaltene subfractions.

A good estimate of the shape of the Athabasca bitumen molar mass distribution has been obtained from PDMS (Larsen and Li, 1995), and is given in Figure 10. We assume that the molar mass distribution of the extracted asphaltenes has the same shape as the portion of the bitumen distribution greater than 400 g/mol. Therefore, the fitting parameters α and β used in Eq. 11 can be obtained directly from the experimental data in Figure 10 and are 50.63 and 0.00165 mol/g, respectively. It remains to determine the range of molar masses present in the asphaltene distribution, i.e., the values of M_L and M_H.

The average molar masses for the soluble (lowest molar mass end of distribution) and insoluble (highest molar mass end) subfractions within the asphaltene can be calculated in the same manner as was the average asphaltene density

$$\overline{M}_{\text{sol}} = \frac{M_i - M_L - \frac{\alpha}{\beta}(\exp\{-\beta M_i\} - \exp\{-\beta M_L\})}{\int_{M_L}^{M_i}\left(\frac{1+\alpha\exp\{-\beta M_i\}}{M_i}\right)dM_i} \tag{18}$$

and

$$\overline{M}_{\text{insol}} = \frac{M_H - M_i - \frac{\alpha}{\beta}(\exp\{-\beta M_H\} - \exp\{-\beta M_i\})}{\int_{M_i}^{M_H}\left(\frac{1+\alpha\exp\{-\beta M_i\}}{M_i}\right)dM_i} \tag{19}$$

Here, $\overline{M}$ is the average molar mass (g/mol). Values of 2,000 and 8,500 g/mol for M_L and M_H were found to best fit the VPO and interfacial tension based estimates of average molar mass, as shown in Figure 9. A molecular thickness of 1.18 nm was used in Eq. 2 to scale the molar masses calculated

from the interfacial tension data to those from VPO experiments. A thickness of 1.18 nm is consistent with molecular dimensions.

Molar volume and solubility parameter correlations

Molar volume is the ratio of molar mass to density. As discussed previously, density was related to molar mass as follows

$$\rho_i = 0.017M_i + 1{,}080 \tag{20}$$

and therefore

$$\nu_i = \frac{1{,}000M_i}{0.017M_i + 1{,}080} \tag{21}$$

The solubility parameter can also be correlated to molar mass with the use of Eq. 6. To the extent that the asphaltenes are a series of polyaromatic hydrocarbons with smoothly increasing aromaticity and with randomly distributed associated functional groups, they can be treated as a homologous series. For a homologous series, the enthalpy of vaporization is a linear function of molar mass as shown in Figure 11. Assuming such a linear function for asphaltenes, the solubility parameter may be expressed as follows

$$\delta_i^l = \left(\frac{\Delta H_i^{\text{vap}} - RT}{\nu_i}\right)^{1/2} = \left(\frac{AM_i + B - RT}{M_i/\rho_i}\right)^{1/2} \tag{22}$$

where ΔH_i^{vap} is the molar enthalpy of vaporization, and A and B are the linear fit parameters for the enthalpy of vaporization vs. molar mass. For high molar mass material such as asphaltenes, the term $B - RT$ has a magnitude in the order of -3 kJ/mol compared with a minimum value of 400 kJ/mol for the AM_i term. Therefore, the $B - RT$ term can be neglected and the following expression results from Eq. 22

$$\delta_i^l \cong (A\rho_i)^{1/2} \tag{23}$$

While A is a physically meaningful parameter, its value is not known and must be determined indirectly from solubility data. However, given that asphaltene aromaticity increases with increasing molar mass, one expects the value of A to be nearer that of the naphthalenes, 398 J/g than the alkanes, 270 J/g.

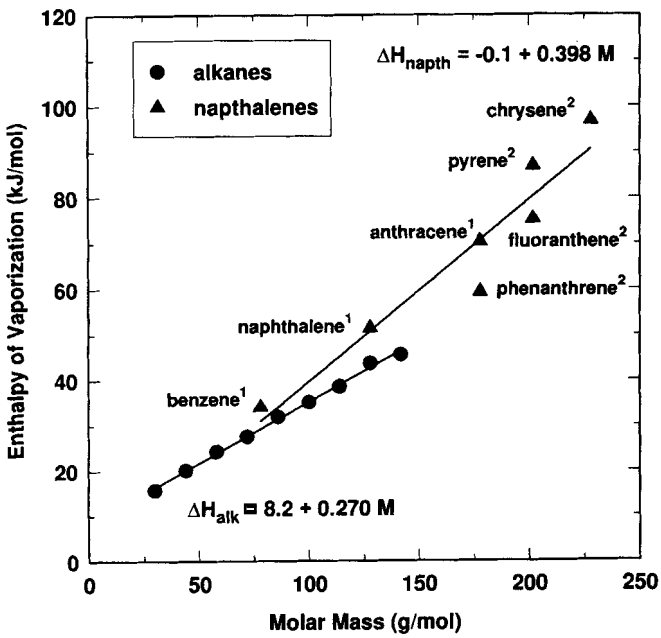

Figure 11. Enthalpy of vaporization of homologous series.

(1) Weast (1978); (2) Daubert and Danner (1985).

Solubility model

Solid-liquid equilibrium calculations were performed using equilibrium ratios determined from Eq. 7. The ratio of the standard state fugacities (Eq. 4) was assumed to be near unity for asphaltenes in toluene-hexane mixtures. The assumption is based on two observations. First, the asphaltenes do not appear to precipitate in a crystalline form, but rather as an amorphous, highly solvated, solid. Indeed, the solid material takes several days to dry out, and seems to crystallize only after most of the solvent has evaporated. The enthalpy of fusion at the point of precipitation may well be small in such circumstances. Secondly, good solubility predictions are obtained when the standard state fugacity ratio is assumed to be near unity and the first term in the exponent of Eq. 7 is neglected.

Solvent solubility parameters of 18.25 for toluene and 14.9 for hexane were obtained from Barton's 1983 Handbook. The mixture solubility parameter is the volume average of the solvent parameters. Densities, molar volumes, and solubility parameters were estimated with Eqs. 20, 21 and 23, respectively, based on the molar mass distribution obtained in Eq. 12. As discussed previously, the parameter A in Eq. 23 was adjusted until the predicted fractional solubilities agreed with experimental data. A value of 367 J/g was found to give the best results. As expected, this value is quite close to the naphthalene value of 398 J/g. Furthermore, the calculated solubility parameters ranged in value from 20 for the smallest asphaltene molecule to 21 for the largest, in good agreement with literature values near 20 (Andersen, 1992). Model predictions are compared with experimental results as an asphaltene concentration of 8.8 kg/m^3 in Figure 12.

In order to illustrate the significance of the first-order density correlation, a zero-order prediction was made assuming a constant asphaltene density of 1,162 kg/m^3 with the results shown in Figure 12. The use of constant density introduces significant errors in the prediction of both the precipitation point and the amount of precipitated material. Using the zero-order density model is equivalent to using a constant value for the asphaltene solubility parameter. Hence, the comparisons in Figure 12 indicate that a small variation in the solubility parameter with molar mass can significantly affect the accuracy of solubility calculations. A density correlation of at least first order is essential to predict the solubility of asphaltenes with acceptable accuracy.

The first-order model agrees reasonably well with the experimental data and predicts fractional precipitation to within 0.02 except near the precipitation point. The precipitation

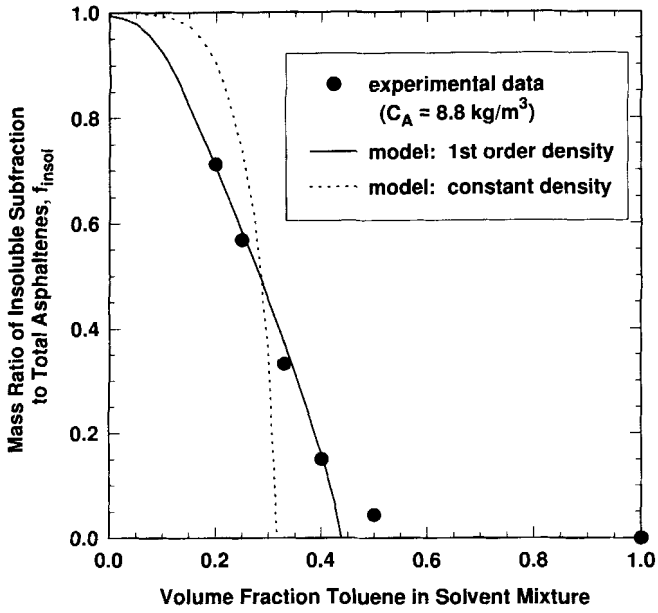

Figure 12. Predicted and experimental solubility of asphaltenes in solutions of toluene and hexane.

point is underestimated by 0.07. Similar accuracy is obtained for an asphaltene-solids concentration range of 1.76 to 17.6 kg/m^3, as shown in Figure 2. Considering the assumptions used to obtain the correlations employed in the model, this level of agreement is fairly good.

Conclusions

For the purpose of solubility calculations, the chemistry of asphaltenes can be estimated by treating asphaltenes as a series of polyaromatic hydrocarbons with randomly distributed associated functional groups. The molar mass distribution for asphaltenes can be obtained with interfacial tension measurements together with VPO data and PDMS data. Molar volume and the solubility parameter for the asphaltenes can be correlated to molar mass. Solubility can be modeled using a solid-liquid equilibrium calculation with K-values derived from Scatchard-Hildenbrand solubility theory incorporating the Flory-Huggins entropy of mixing.

The resulting multicomponent equilibrium calculation was tested on solutions of toluene and hexane. In this case there was one estimated parameter, the rate at which the asphaltene enthalpy of vaporization changes with molar mass. The value of the parameter used in the model was within 10% of that for the naphthalenes. The solubility model predicted the precipitation point to within 0.07 of the hexane volume fraction required and predicted the fractional amount of precipitate to within 0.05 across a broad range of concentrations and toluene/hexane ratios. The small variation in asphaltene solubility parameter with molar mass resulted in significantly improved predictions compared with a constant solubility parameter model. The correlations used here need to be tested for their robustness on asphaltenes from other sources and with different solvents.

Notation

A, B = linear fit parameters for enthalpy of vaporization molar mass correlation
$Cppt$ = solubility limit (kg/m^3)
f = mass ratio of asphaltene subfraction to total asphaltene fraction
f^* = mass ratio of asphaltene-solids subfraction to total asphaltene-solids mixture
K = equilibrium ratio

Acknowledgments

We thank Syncrude Canada Ltd. and the Natural Sciences and Engineering Research Council of Canada for financial support. We are also indebted to D. Mahlow and Drs. M. R. Gray, Y. Maham and A. E. Mather for their assistance.

Literature Cited

Acevedo, S., G. Escobar, L. Gutierrez, and H. Rivas, "Isolation and Characterization of Natural Surfactants from Extra Heavy Crude Oils, Asphaltenes and Maltenes: Interpretation of Their Interfacial Tension-pH Behavior in Terms of Ion Pair Formation," *Fuel*, **71**, 619 (1992).

Andersen, S. I., "Effect of Precipitation Temperatures on the Composition of *N*-Heptane Asphaltenes," *Fuel Sci. Technol. Intl.*, **12**(12), 51 (1994).

Andersen, S. I., "Hysteresis in Precipitation and Dissolution of Petroleum Asphaltenes," *Fuel Sci. Technol. Int.*, **10**(10), 1743 (1992).

Barton, A. M. F., *CRC Handbook of Solubility Parameters and Other Cohesion Parameters*, CRC Press, Boca Raton, FL (1983).

Brandt, H. C. A., E. M. Hendriks, M. A. J. Michels, and F. Visser, "Thermodynamic Model of Asphaltene Stacking," *J. Phys. Chem.*, **99**, 10430 (1995).

Brons, G., "Solvent Deasphalting Effects on Whole Cold Lake Bitumen," *Energy & Fuels*, **9**, 641 (1995).

Cimino, R., S. Correra, E. Sacomani, and C. Carniani, "Thermodynamic Modelling for Prediction of Asphaltene Deposition in Live Oils," *SPE Int. Symp. Oilfield Chemistry*, San Antonio (Feb. 1995).

Cyr, N., G. McIntyre, G. Toth, and O. P. Strausz, "Hydrocarbon Structural Group Analysis of Athabasca Asphaltene and its G.P.C. Fractions by ^{13}C.N.M.R.," *Fuel*, **66**, 1709 (1987).

Daubert, T. E., and R. P. Danner, "Data Compilation Tables of Properties of Pure Compounds," AIChE, New York (1985).

Ferworn, K. A., and W. Y. Svercek, "Thermodynamic and Kinetic Studies of Asphaltene Deposition from Bitumens," *Proc. Can. Chem. Eng. Conf.*, Calgary (Oct., 1994).

Harkins, W. D., and H. F. Jordan, "A Method for the Determination of Surface and Interfacial Tension from the Maximum Pull on a Ring," *J. Amer. Chem. Soc.*, **52**, 1751 (1930).

Hirschberg, A., L. N. J. deJong, B. A. Schipper, and J. G. Meijer, "Influence of Temperature and Pressure on Asphaltene Flocculation," *SPE J.*, **24**, 283 (1984).

Kawanaka, S., S. J. Park, and G. A. Mansoori, "Organic Deposition from Reservoir Fluids: A Thermodynamic Predictive Technique," *SPE Res. Eng.*, **5**, 185 (1991).

Larsen, J. W., and S. Li, "Determination of Bitumen Molecular Weight Distributions Using ^{252}Cf Plasma Desorption Mass Spectrometry," *Energy & Fuels*, **9**, 760 (1995).

Lira-Galeana, C., A. Firoozabadi, and J. M. Prausnitz, "Thermodynamics of Wax Precipitation in Petroleum Mixtures," *AIChE J.*, **42**, 239 (1996).

Mehrotra, A. K., M. Sarkar, and W. Y. Svrcek, "Bitumen Density and Gas Solubility Predictions Using the Peng-Robinson Equation of State," *AOSTRA J. Res.*, **1**(4), 215 (1985).

Moschopedis, S. E., J. F. Fryer, and J. G. Speight, "Investigation of Asphaltene Molecular Weights," *Fuel*, **55**, 227 (1976).

Prausnitz, J. M., R. N. Lichtenthaler, and E. G. de Azevedo, *Molecular Thermodynamics of Fluid-Phase Equilibria*, 2nd ed., Prentice-Hall, Englewood Cliffs, NJ (1986).

Rassamdana, H., B. Dabir, M. Nematy, M. Farhani, and M. Sahimi, "Asphalt Flocculation and Deposition: I. The Onset of Precipitation," *AIChE J.*, **42,** 10 (1996).
Sheu, E. Y., M. M. De Tar, and D. A. Storm, "Interfacial Properties of Asphaltenes," *Fuel*, **71,** 1277 (1992).
Speight, J. G., and S. E. Moschopedis, "Some Observations on the Molecular Nature of Petroleum Asphaltenes," *Preprints, Div. of Fuel Chem., ACS*, **24,** 910 (1979).
Strausz, O. P., T. W. Mojelsky, and E. M. Lown, "The Molecular Structure of Asphaltene: an Unfolding Story," *Fuel*, **71,** 1355 (1992).
Taylor, S. E., "Use of Surface Tension Measurements to Evaluate Aggregation of Asphaltenes in Organic Solvents," *Fuel*, **71,** 1338 (1992).
Thomas, F. B., D. B. Bennion, and D. W. Bennion, "Experimental and Theoretical Studies of Solids Precipitation from Reservoir Fluid," *J. Cnd. Petr. Tech.*, **31**(1), 22 (1992).
Weast, R. C., *CRC Handbook of Chemistry and Physics*, 59th ed., CRC Press, Boca Raton, FL (1978–79).

Manuscript received Mar. 4, 1996, and revision received May 21, 1996.